The 2020 World Congress on
The 2020 Structures Congress (Structures20)
25-28, August, 2020, GECE, Seoul, Korea

Geometrical and mechanical optimization of shear connectors for CFS-concrete composite systems

*Xavier Fernando Hurtado Amézquita[1)] and Maritzabel Molina Herrera[2)]

[1) 2)] Universidad Nacional de Colombia, Bogotá, Colombia
[1)] Universidad de la Salle, Bogotá, Colombia
xfhurtadoa@unal.edu.co, mmolinah@unal.edu.co

ABSTRACT

Over the past 20 years, the use of Cold-Formed Steel (CFS) and concrete composite sections has increased its application, mainly in medium and small structures. The most important advantages of these construction systems are high load-bearing capacity, high stiffness and ductility, full usage of the capacity of the materials, and they are considered economic systems and an alternative for sustainability in construction.

Previous researches about light-steel composite sections have aimed to explore different alternative fastening systems to fix connectors by avoiding welding, proposing new configuration of shear connectors, and evaluating the contribution of additional elements in the system capacity, such as reinforcing bars and concrete dowels, to improve the system performance.

In this research, a new configuration of shear connector for CFS sections is proposed. The computational models were performed and analyzed by applying the finite element method, which involves non-linear properties of the materials and the interaction between them.

A Central Composite Face-Centered (CCF) statistical design was arranged to execute the most representative analysis configurations of geometric variables in the analytical models. Additionally, mechanical optimization was carried out by applying response surface methodology (RSM), reaching the configuration with the best structural performance.

1. INTRODUCTION

Over the past 20 years, the use of Cold-Formed Steel (CFS) and concrete composite sections has increased its application, mainly in medium and small structures (Bamaga, 2012). The most important advantages of these construction systems are high load-bearing capacity, high stiffness and ductility and full usage of capacity of the materials, thus they have been considered as economic systems and an alternative for sustainability in construction (Irwan et al., 2009; Lawan et al., 2015, Alhajri et al., 2016).

[1)] Research Student, Ph.D. School of Civil Engineering. - Assistant Professor, Department of Civil Engineering
[2)] Associate Professor, Department of Civil Engineering

Current code formulations to design shear connectors in composite systems have been validated by experimental studies on Hot Rolled Steel (HRS) sections, which are not efficient in CFS sections due to restrictions caused by their limited thickness. Moreover, any proposal on shear connectors must be supported by experimental tests and analytical studies, in order to guarantee adequate system behavior.

Fastening mechanisms of shear connectors have been one of the most critical aspects of CFS shapes. Therefore, welding becomes an inefficient process because the steel plate can be burned and perforated, reducing the capacity of composite systems. In this way, some researchers studied alternative fastening systems for CFS sections, avoiding welding.

Performance of predrilled bolted shear connectors (Fig. 1.a) was studied by Hanaor (2000), Lakkavalli & Liu (2006), Queiroz el at. (2010), Wehbe et al. (2011) and Lawan et al. (2015). Ductile behavior was evidenced in this configuration, reaching up to 95% of maximum load in conventional welded stud systems. Increases in bolt diameter improved bearing loads in composite systems (Lawan et at. 2015). Initial movements were recorded due to bolt-hole clearance. In this way, Pathirana et al. (2016) recommended using expansive collar and washers to reduce the possibility of early displacements of samples, induced during initial loading. (Fig. 1.b)

Researches on composite systems with self-drilling screws (Fig. 1.c) have been developed by Hanaor (2000), Lakkavalli & Liu (2006), Bamaga et al. (2012), Merryfield et al. (2016) and Kyvelou et al. (2018). Although this composite configuration became an efficient system due to the high fixation, the limited capacity of each screw implies installing a large number of connectors. Therefore, the use of self-drilling shear as shear connectors may be an impractical solution for building composite members.

a) b) c)

Fig. 1. a). Bolted shear connectors (taken from Queiroz et al. 2010). b). Proposal to restrict early displacements (taken from Pathirana et al. 2016). c). Self-drilling screws shear connectors (taken from Lakavalli & Liu 2006).

Hsu et al. (2012) also used self-drilling screws to join an innovative element denominated cold-formed furring shear connector (Fig. 2). This system was composed of a continuous hat channel, placed on the steel beam and embedded into the concrete slab. Majdi et al. (2014) validated the system behavior through numerical analysis by applying the finite element method, evidencing high ductility in bending beam tests, as well as the separation between materials, becoming non-composite systems.

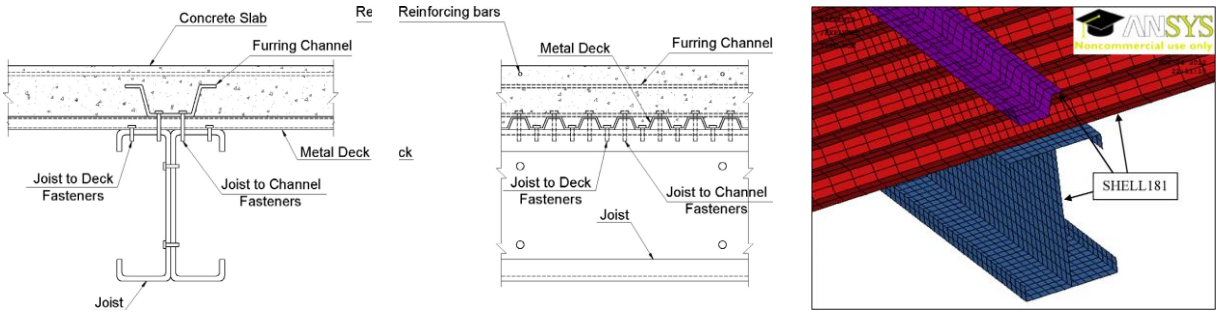

a). b). c).

Fig. 2. Continuous furring channel used as shear connector: a) and b) General arrangement (taken from Hsu et al., 2012), c) Finite element model (taken from Majdi et al., 2014).

Powder-actuated nails were applied as a fastening mechanism in different proposals of shear connectors. Arroyo et al. (1997) proposed an alternative stud, which was patented as SPIT (Fig. 3.a). In this connector, the support base was extended, distributing stresses in the interface in a better way in comparison to conventional welded studs. These elements allowed to develop a ductile behavior in the composite system. Fontana & Bärtschi (2002) developed different custom configurations of shear connectors by bending and cutting cold-formed steel plates, called rib connectors (Fig. 3.b). Derlatka et al. (2019) analyzed the effectiveness of top-hat shear connectors in push-out tests, which were initially proposed by Lawson et al. (2001) (Fig. 3.c). In general, most of the failure modes were associated with rotation and cutting in steel nails and tearing in shear connectors, with previous excessive deformations, decoupling the composite system. In addition, Derlatka et al. (2019) studied the effect of the connector length, concluding that longer connectors induce less bearing loads.

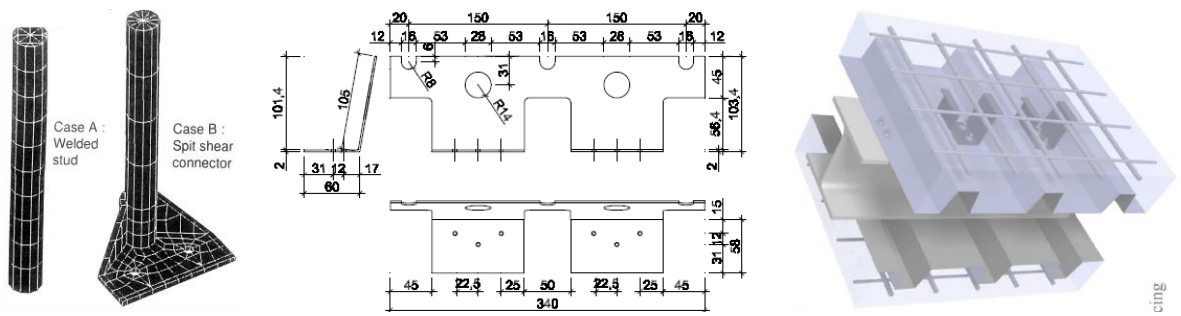

a). b). c).

Fig. 3. a). SPIT shear connector (taken from Arroyo et al. 1997). b). Rib shear connector (taken from Fontana & Bärtschi 2002). c). Top-hat shear connectors (taken from Derlatka et al. 2019).

Contribution of additional elements in the system capacity, such as reinforcing bars and concrete dowels, were studied by Costa-Neves et al. (2013) and Liu et al. (2015), respectively. Experimental results have demonstrated that the incorporation of reinforcing bars and concrete dowels improves the whole capacity of the composite

system, allowing larger displacements and higher loads. Moreover, tensile stresses in bars reduce the possibility of early cracking in the concrete slab and induce its spread on the surface. In the same way, the size and geometry of concrete dowels affect the bearing resistance of the composite system.

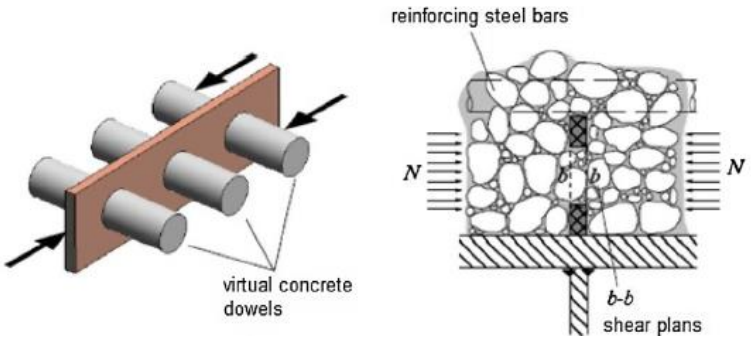

Fig. 4. Reinforced steel bars and concrete dowels: Working principle (taken from Costa-Neves et al. 2013).

Numerical models have been widely used in simulation tests of steel-concrete composite structures. Fig. 5 shows the most representative tests to evaluate interaction capacity.

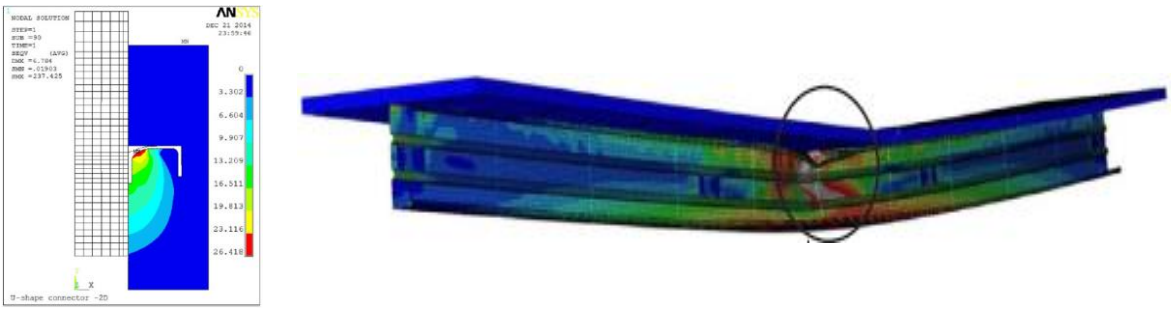

a) b)

Fig. 5. Experimental test of computational simulation: a) Push-out test (taken from Titoum et al. 2016) and b) full-scale beam test (taken from Kyvelou et al. 2018).

Depending on the scope of the research, analytical procedures can predict non-linear responses and ultimate load capacities as an alternative to such an expensive experimental test. Moreover, all results can be meticulously verified, but it is important to check analytical methods against well-controlled selective experimental results.

In this research, a new configuration of shear connector is proposed for CFS sections. The computational models were analyzed by applying the finite element method, which involves non-linear properties of the materials and the interaction between them.

A Central Composite Face-Centered (CCF) statistical design (Montgomery 2013) was arranged to execute the most representative analysis configurations of geometrical variables in analytical models. Additionally, mechanical optimization was carried out by

applying the Response Surface Methodology (RSM) (Montgomery, 2013), reaching the configuration with the best structural performance.

2. DESCRIPTION OF MODELS

2.1. Description of specimens and shear mechanism

ANSYS Workbench was the software selected to simulate the mechanical behavior of the specimens. All components were modeled using 3D quadratic elements for more accurate results.

The whole analytical model was composed of a new proposal for shear connector and reinforcement bar embedded into a 400mm x 300mm x 100mm concrete slab. (Fig. 6). Self-drilling screws for mechanical fastening were also included in the structural model. The internal elements were subtracted from the concrete block to be replaced by steel pieces.

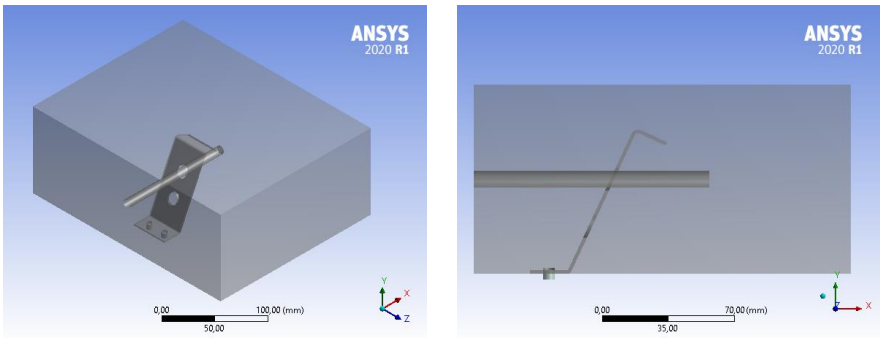

a) b)

Fig. 6. Structural simulation model: a) 3D view. b) Front view.

The geometry of the shear connector was defined according to the following criteria:

- Self-drilling screws as a fastening mechanism due to the final behavior in previous experimental tests.
- Connectors made of cold-formed steel plates in order to have similar stiffness with respect to CFS shapes.
- Curved element to guarantee mechanical fixation to the concrete matrix, increasing lateral stiffness.
- Low cost in the construction process.
- Concrete dowels induced by perforations in the connector, and addition of reinforcing bars to reduce cracking in the concrete slab.

A mechanical model for concrete dowel was initially proposed by Kraus & Wurzer (1997), and adapted by Liu et al. (2016), as shown in (Fig. 7). According to Liu et al. (2016), the shear force is transmitted from the connector to the concrete by contact at the hole edge. The load spreads below the contact surfaces, mainly in zone A and zone B. The concrete in zone A is under triaxial compression, where crushing occurs. In zone B, compression acts along the direction of load spread, while tension acts transversely.

Cracking occurs in zone B when the transverse stresses exceed the concrete tensile strength. The shear connector failure occurs on inclined surfaces due to crushing and cracking of concrete. The reinforcing rebar in the hole increases the confining effect in zone A and receives the tensile forces in zone B, which leads to a large increase in the shear capacity of the connector. (Liu et al. 2016)

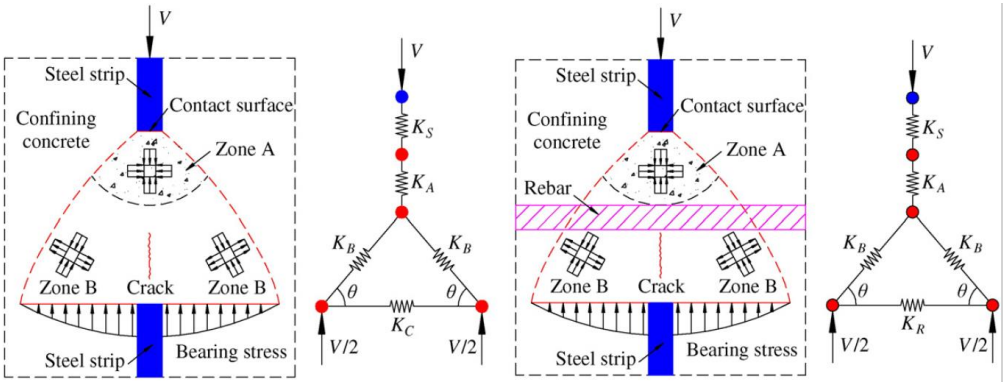

a) b)

Fig. 7. Shear transfer mechanism: a) No rebar in hole (taken from Liu et al. 2016). b) Rebar in hole (taken from Liu et al. 2016).

2.2. Materials

The material properties of the components of the finite element models were represented by constitutive laws and their nominal properties.

<u>Concrete</u> The non-linear behavior of concrete was characterized as multi-linear isotropic hardening by an equivalent uniaxial stress-strain curve of concrete (Fig. 8. a), which uses Von Misses yield criterion. The relationship between compression stress and the strain was taken from Eq. (1) and Eq. (2). The compression was assumed to be linear elastic up to 0.40 f'_c. The negative gradient in the last stage of the stress-strain curve was not taken into account.

$$\sigma_c = \frac{f'_c \gamma \left({\varepsilon_c}/{\varepsilon'_c} \right)}{\left[\gamma - 1 + \left({\varepsilon_c}/{\varepsilon'_c} \right)^{\gamma} \right]} \tag{1}$$

$$\gamma = \left(\frac{f'_c}{32.4} \right) + 1.55 \tag{2}$$

where f'_c is the nominal compressive strength of concrete, σ_c is the uniaxial compression stress and ε_c is the uniaxial strain of the concrete. ε'_c is the maximum strain at the maximum stress, defined as 0,0025.

<u>Steel</u> For all the elements, steel material was modeled as elastoplastic, using the bilinear curve as shown in (Fig. 8. b), considering small hardening for convergence. Nominal properties are presented in Table 1.

Table 1. Nominal mechanical properties of steel components.

		Shear connector (ASTM A424 - Type II) [MPa]	Self-drilling screw fastener (ASTM A449) [MPa]	Steel reinforcement (ASTM A706) [MPa]
Modulus of elasticity	*(Ec)*	200.000	200.000	200.000
Yield stress	*(fy)*	240	644	420
Ultimate tensile stress	*(fu)*	350	840	560

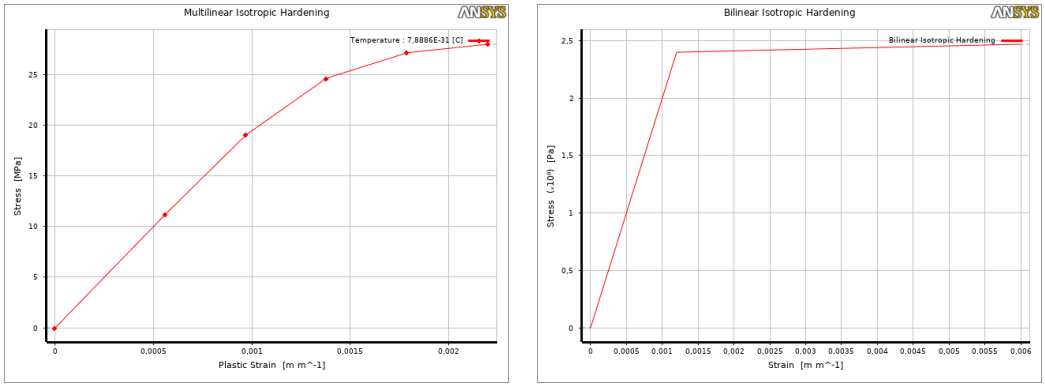

a) b)

Fig. 8. Uniaxial stress-strain relationship for different materials: a) Concrete. b). Steel.

2.3. Interaction and boundary conditions

Due to the symmetry of the specimen, only half of the system was modeled in the analysis, in order to reduce the simulation time. Therefore, all nodes along the symmetry plane of the concrete slab and reinforcing bar were restricted from moving in the X direction (Fig. 9.a).

Screw fasteners were considered as fixed supports, thus all degrees of freedom (DOFs) were restricted. Moreover, all nodes at the base of the concrete slab were restricted from moving in the Y direction, avoiding rotations in the specimen (Fig. 9.a).

The monotonic load was applied as enforced lateral displacement on the concrete slab in the Z direction. Due to the limited movements in the system, large displacements were not considered. (Fig. 9.a).

Interaction among different elements was modeled by using frictional contacts, to represent the behavior of the surfaces in the specimen components, avoiding free slips among elements. The value for the frictional coefficient was assumed to be 0.20 between the steel elements and the concrete slab surface, and 0.80 between fasteners and shear connector due to the high connection evidenced in previous experimental tests. (Fig. 9.b).

The unsymmetric Newton Raphson method was applied to solve non-linear equations according to the user guide of the ANSYS manual. The software performs an iterative approach to obtain equilibrium in each increment in displacement.

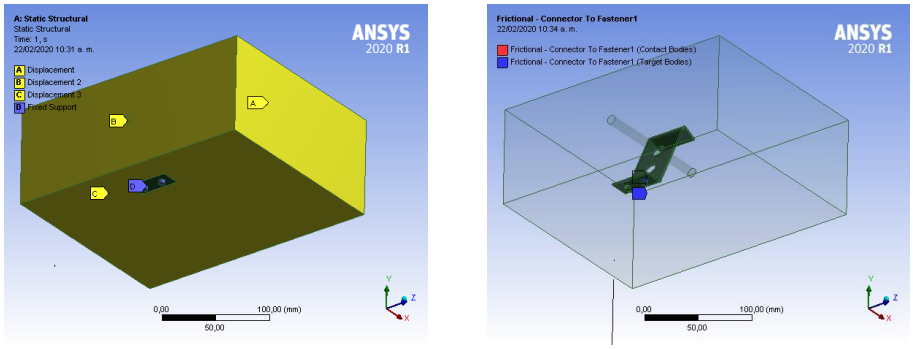

a) b)

Fig. 9. a) Boundary conditions in the whole specimen. b) Contact interaction among different elements.

2.4. Meshing

The discretization of each element of the model was made by applying a coarse adaptative mesh. The fine mesh was applied at the connector, the reinforcing bar and the fasteners areas to obtain more accurate results. The overall mesh size was around 20mm and was reduced to 2mm on contact surfaces, where a high gradient was expected (Fig. 10).

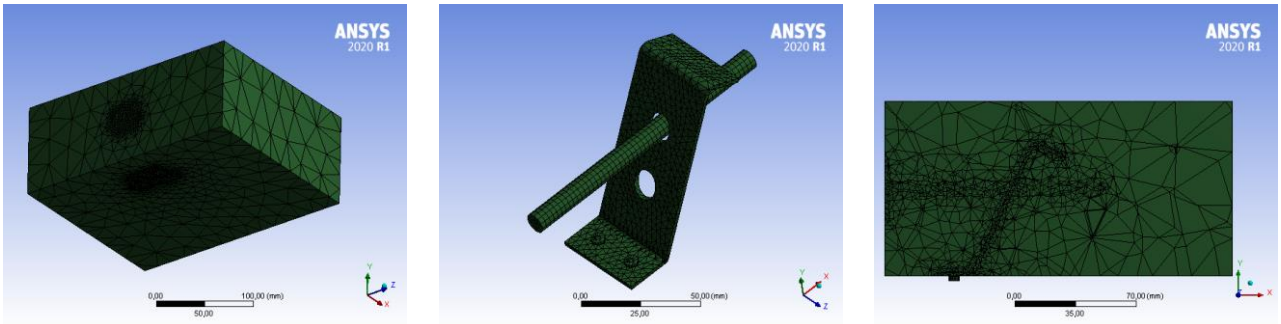

a) b) c)

Fig. 10. Specimen mesh model: a) Whole slab concrete. b) Steel elements. c) Middle cross section.

3. STATISTICAL DESIGN OF EXPERIMENTS

The Central Composite Face-Centered (CFC) design was selected to evaluate the contribution of study variables in the system behavior, allowing second-order fittings. In this case, the inclination angle and connector thickness were defined as relevant geometric variables. Study levels are listed in Table 2.

Table 2. Description of study variables and levels.

Variable 1	Level	Variable 2	Level
Angle	40°	Thickness	1.5mm
	50°		1.6mm
	60°		1.7mm
	70°		1.8mm
	80°		1.9mm
	90° (Vertical position)		

Furthermore, a range of displacements was limited from 0.01mm to 0.09mm, which guarantees the behavior of the material under the nominal stress limit.

Based on the methodology, Table 3 lists the specific design points from the whole experimental matrix that were selected for testing. Fig. 11 shows the graphic selection of design points. Values +1 and -1 indicate coded variables between maximum and minimum values in the natural variables (x1, x2 and x3), respectively.

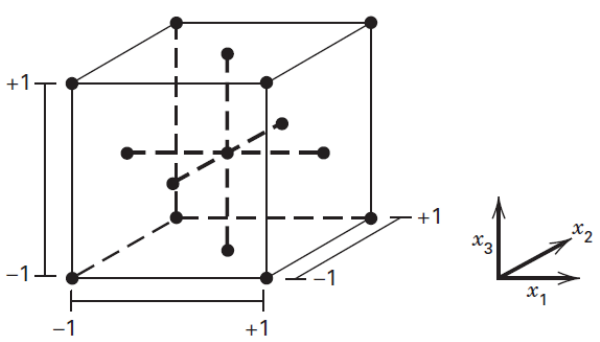

Fig. 11. Central Composite Face-centered design: Identification of design points (taken from Montgomery 2013).

Table 3. Results of experimental design points

Design point	Designation model	Thickness (x1)	Inclination Angle (x2)	Displacement (x3)	Maximum load reaction	Maximum stress in concrete slab	Maximin stress in steel connector
		[mm]	[deg]	x10^{-2} [mm]	[kN]	[MPa]	[MPa]
1	M65-17-5	1.7	65°	5	-6.42	27.72	251.62
2	M65-15-5	1.5	65°	5	-6.22	27.48	245.79
3	M65-19-5	1.9	65°	5	-6.82	27.74	250.89
4	M65-17-9	1.7	65°	9	-9.26	27.80	273.13
5	M65-17-1	1.7	65°	1	-1.68	17.90	174.03
6	M90-17-5	1.7	90°	5	-6.46	27.87	246.33
7	M90-17-5	1.7	40°	5	-6.27	27.89	255.92
8	M90-15-9	1.5	90°	9	-8.25	27.89	281.80

9	M90-19-9	1.9	90°	9	-9.86	27.74	266.29
10	M90-15-1	1.5	90°	1	-1.41	26.22	85.17
11	M90-19-1	1.9	90°	1	-1.63	18.50	149.44
12	M40-15-9	1.5	40°	9	-8.85	27.73	298.35
13	M40-19-9	1.9	40°	9	-9.67	27.85	287.76
14	M40-15-1	1.5	40°	1	-1.74	26.76	221.61
15	M40-19-1	1.9	40°	1	-1.62	19.74	142.58

The Surface Response Methodology (RSM) allows to develop a mathematical and statistical model to correlate the variables with effects of interest, in this case the maximum reaction force, the maximum stresses in the materials and the controlled displacements. Likewise, the optimal response can be obtained, thus guaranteeing the best results within the study limits.

4. RESULTS AND DISCUSSION

The evaluated surface responses are shown in Fig. 12, for the specific effects, previously indicated. The summarized results of the response effects are given in Table 3.

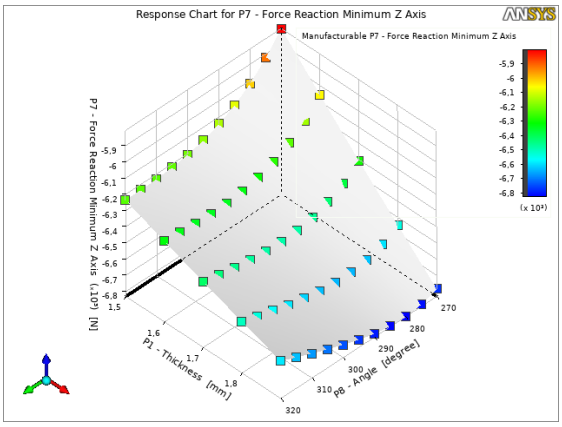

a).

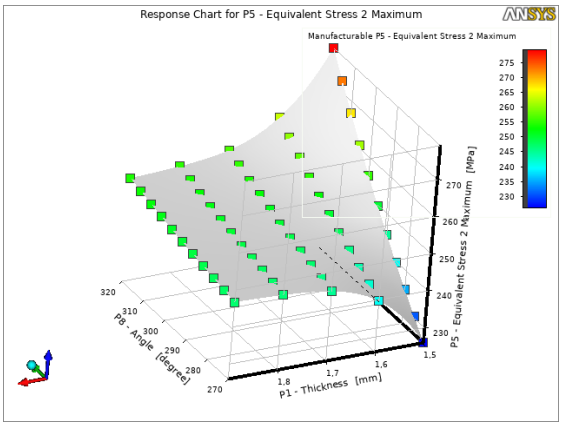

b).

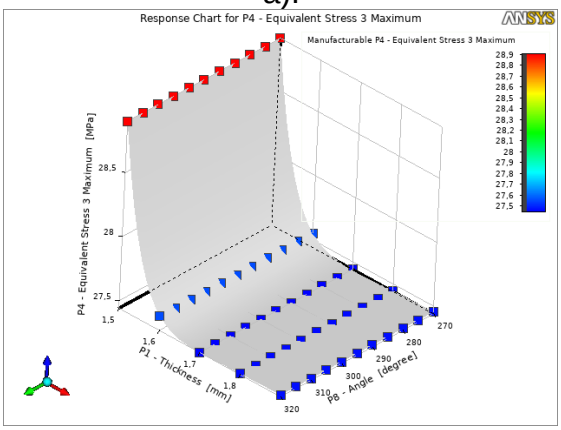

c).

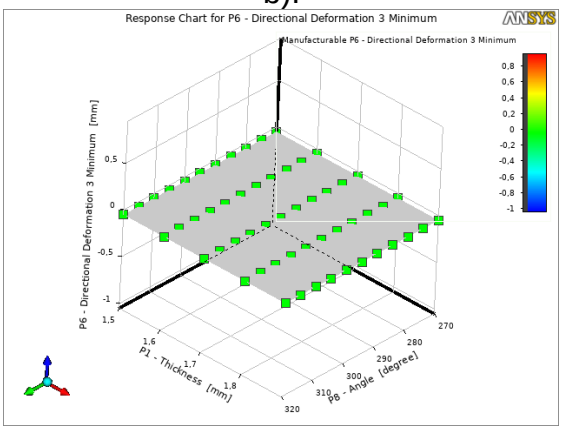

d).

Fig. 12. Surface response for inclination angle and thickness variation: a) Reaction force. b) Stress on steel connector. c) Stress on concrete slab. d) Displacements.

4.1. Parametric studies

Thickness effect A thickness range between 1.5mm and 1.9mm was evaluated, according to commercial information of the ASTM A424 steel plates (Table 2). Fig. 12 shows that reaction forces increase as thickness increases, while material stresses decrease. This behavior occurs in all models, mainly at high inclinations.

Inclination angle effect An inclination angle range between 40° and 90° was selected to ensure construction facilities (Table 2). Therefore, connector dimensions and hole size perforations were aimed to be fabricated by hand. Moreover, the minimum inclination corresponds to the ease to flow of fresh concrete during pouring, avoiding holes in the concrete matrix.

The angle variation indicates that the more vertical the connector, the higher force reaction is obtained with higher thickness, and stresses stabilize without representative changes in behavior. However, models with lower thickness have an opposite effect with wide variations in steel stresses and reduced stresses in the concrete slab. Furthermore, smaller inclinations induce higher reaction forces.

4.2. *Optimization*

The selected optimization method was the Multi-Objective Genetic Algorithm (MOGA), which supports multiple objectives and constraints and aims to find the global optimum. Therefore, according to the established limits, the optimal behavior occurs in composite systems with *1.9 mm shear connectors inclined 65°*. Consequently, the results presented in the following sections are focused on characterizing this optimized configuration (M65-19-4).

4.3. *Force-Displacement behavior*

The reaction load vs. displacement curve is obtained by an iterative procedure over each displacement increment, where software has to satisfy equilibrium (Fig. 13).

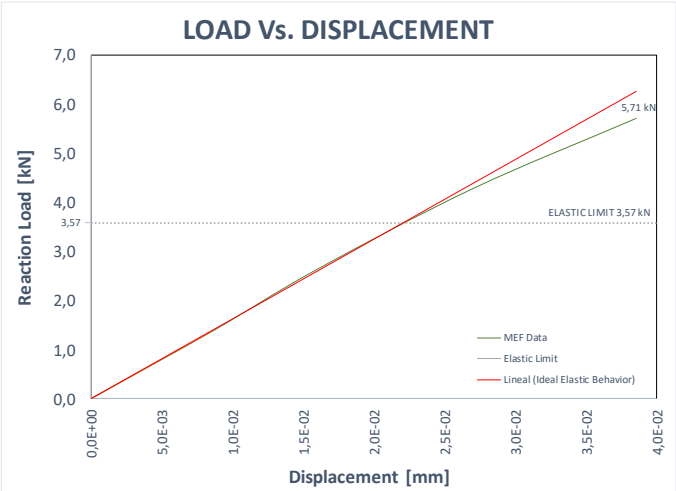

Fig. 13. Reaction load vs. displacement curve in specimen M65-19-4.

Data logging was recorded up to the failure load. The descending branch, associated with stiffness degradation, was not recorded due to the selected constitutive model of concrete.

The tendency of the curve shows that the elastic limit was exceeded over 60%, thus developing inelastic behavior. However, due to the limited displacements achieved, this new type of shear connector is considered as a rigid connector, according to the limit established by the Eurocode 4, that is, greater than 6mm.

The state of the final displacements is presented in Fig. 14. Displacements show an increase as the element fibers move away from the connector fastening point, particularly at the base of the composite system.

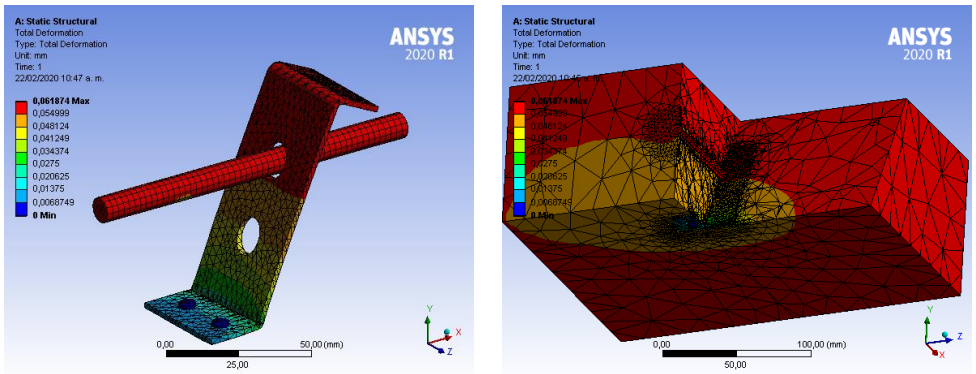

a) b)

Fig. 14. Displacements of the final state in specimen M65-19-4: a) Steel elements. b) Concrete slab.

4.4. Stresses

Fig. 15 presents the graphic results of stress behavior. Fig. 15. a) and Fig. 15. b) show the final state of the concrete slab. In both figures, compression areas are identified. Shear connector induces high stresses at the base, near to the fastening system, causing crushing and sliding in the zone around the connector. In the reinforcing area, transference stresses are evident, which guarantees the efficiency of including a steel bar into the composite system.

Fig. 15. c) shows the final stress state in steel elements. A high concentration of stresses is in the fastening areas. All stress values were below the nominal strength capacity.

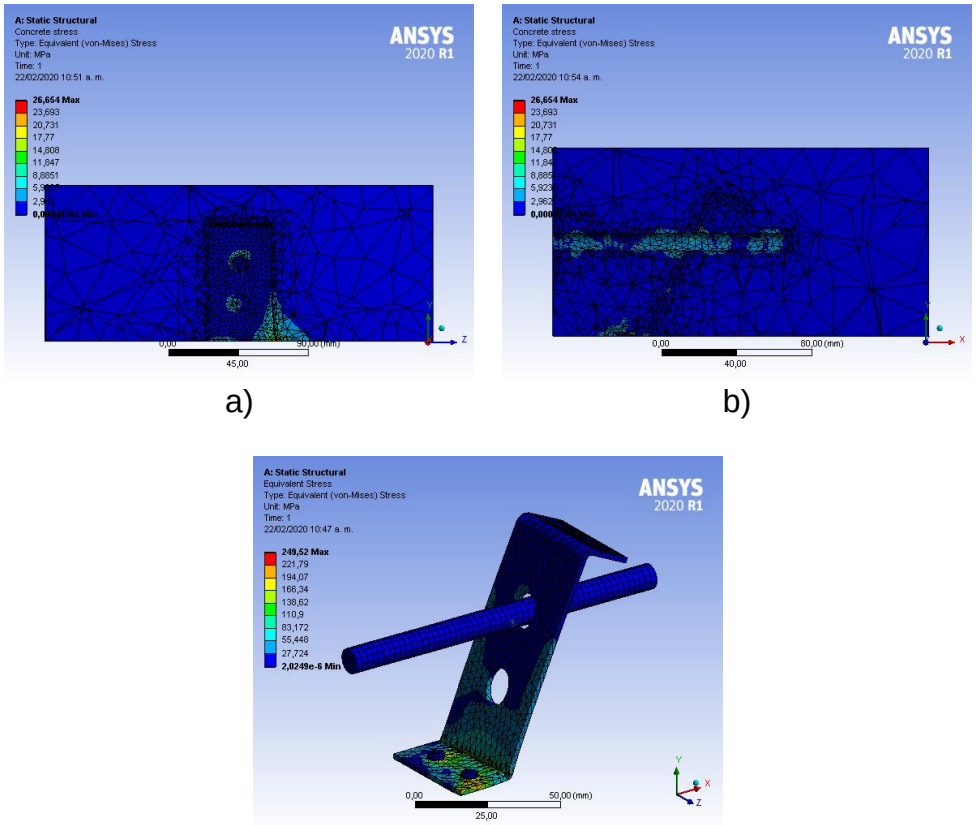

Fig. 15. Stress state in specimen M65-19-4: a) Concrete slab. b) Cross section. c) Steel elements.

5. CONCLUSIONS

In this paper, a non-linear finite element model was performed to simulate the mechanical behavior of a new shear connector proposal. The geometric and structural configuration of the system took into account the feasibility of the fabrication and installation of steel pieces, as well as constructive procedures during concrete pouring.

The thickness and the inclination angle were selected as the most representative variables in the behavior of the composite system. Parametric studies concluded that the system performance improves by increasing their physical values of configuration.

According to FE results, it was possible to evidence the inelastic behavior of the composite system before failure, as well as interaction among all components: shear connector, self-drilling fasteners, reinforcing bar and concrete slab.

By using the response surface methodology, the optimization of the structural system was carried out. As a result, a new configuration was proposed for shear connectors fabricated of ASTM A424 steel plate, the thickness of 1.90mm and the inclination of 65° with respect to the horizontal plane.

REFERENCES

Alhajri, T., Tahir, M., Azimi, M., Mirza, J., Lawan, M., Alenezi, K., & Ragaee, M. (2016). "Behavior of pre-cast u-shaped composite beam integrating cold-formed steel with ferro-cement slab". *Thin-Walled Structures*, **102**, 18–29.

American Institute of Steel Construction. "Specification for structural steel buildings". 2010.

American Iron and Steel Institute. "North american specification for the design of cold-formed steel structural members (S-100)". (2016).

Arroyo, R. & Jullien, J. (1997). "A new shear stud connector proposal". *In 15th International Specialty Conference on Cold-Formed Steel Structures*, 307-319. *In ASCE Structures Congress*, 298-311.

Architectural Institute of Korea. (2014). "Korea building codes (KBC)".

ASM International – The Materials Information Society. (2012). "Sheet metal forming".

Associacao Brasileira de Normas Tecnicas. (2008). "Norma brasileira ABNT 8800".

Australian/New Zeland Standards. (2005). "Cold formed steel structures (AS/NZ 4600:2005)".

Bamaga, S., Tahir, M., & Tan, C. S. (2012). "Push tests on innovative shear connector for composite beam with cold-formed steel section". *In 21st International Specialty Conference on Cold-Formed Steel Structures - Recent Research and Developments in Cold-Formed Steel Design and Construction*, 325–337.

Bamaga, S., Tahir, M. Md., Tan, C. S., Shek, P. N. & Aghlara, R. (2019). "Push-out test on three innovative shear connectors for composite cold-formed steel concrete beams". *Construction and Building Materials*, **223**, 288-298.

British Standard. (2010). "Structural use of steelwork in building".

Canadian Standards Association. (2007). "North american specification for the design of cold formed steel structural members (S136-07)".

Costa-Neves, L., Figueiredo, J., S.Vellasco, P. & Da Cruz, J. (2013). "Perforated shear connectors on composite girders under monotonic loading: an experimental approach". *Engineering Structures*, **56**, 721-737.

Derlatka, A., Lacki, P., Nawrot, J.& Winoviecka, J. (2019). "Numerical and experimental test of steel concrete composite beam with the connector made of top-hat profile". *Composite Structures*, **211**, 244-253.

European Committee Standardization. (2004). "EUROCODE 4: Design of composite steel and concrete structures".

Fontana, M. & Bärtschi, R. (2002). "New types of shear connectors with powder-actuated fasteners". *ETH Zürich Research Collection. Institute of Struictural Engineering – Swiss Federal Institute of Technology Zurich. ETH Library.*

Hanaor, A. (2000). "Tests of composite beams with cold-formed sections". *Journal of Constructional Steel Research*, **54**(2), 245–264.

Hsu, T., Munoz, R., Punurai, S., Majdi, Y., & Punurai, W. (2012). "Behavior of composite beams with cold-formed steel joists and concrete slab". *In 21st International Specialty Conference on Cold-Formed Steel Structures - Recent Research and Developments in Cold-Formed Steel Design and Construcción*, 339–353.

Irvwan, J., & Hanizah, A. (2009). “Test of shear transfer enhancement in symmetric cold-formed steel concrete composite beams”. *Journal of Constructional Steel Research*, **65**, 2087-2098.

Japan Society of Civil Engineers. (2007). “Standard specifications for steel and composite structures”.

Kraus, D. & Wurzer, O. (1997). “Non-linear finite element analysis of concrete dowels”. *Computers & Structures.* **64**, 1271-1279.

Kyvelou, P., Gardner, L. & Nethercot, D, (2018). “Finite element modelling of composite cold-formed steel flooring systems.” *Engineering Structures.* **158**, 28-42.

Lakkavalli, B. & Liu, Y. (2006). “Experimental study of composite cold-formed steel c-section floor joist”. *Journal of Constructional Steel Research*, **62**, 995-1006.

Lawan, M., Tahir, M., Ngian, S. & Sulaiman, A. (2015). “Structural performance of cold-formed steel section in composite structures: a review”. *Jurnal Teknologi*, **74**(4), 165-175.

Lawson, R., Popo-Ola, S. & Varley, D. (2001). “Innovative development of light steel composites in buildings”. *In International union of laboratories and experts in construction materials and structures (RILEM). International symposium on connections between steel and concrete.*

Liu, Y., Zheng, S., Yoda, T. & Liu, W. (2015). “Parametric study on shear capacity of circular-hole and long-hole perfobond shear connector”. *Composite Structures*, **117**, 64-80.

Majdi, Y., Hsu, C. & Zarei, M. (2014). “Finite element analysis of new composite floors having cold-formed steel and concrete slab”. *Engineering Structures*. **77**, 65-83.

Merryfield, G., El-Ragaby, A., & Ghrib, F. (2016). “New shear connector for open web steel joist with metal deck and concrete slab floor system”. *Construction and Building Materials*, **125**, 1-11.

Montgomery, D. (2013). “Design and analysis of experiments”. 8°Ed. Wiley, New Jesey, USA.

Pathirana, S., Uy, B., Mirza, O. & Zhu, X. (2016). “Flexural behavior pf composite steel-concrete beams utilizing blind bolt shear connectors” *Engineering Structures.* **114**, 181-194.

Queiroz, G., Rodrigues, F., Pereira, S., Pfeil, M., Oliveira, C. & Da Mata, L. (2010). “Behavior of steel concrete beams with flexible shear connectors”. *In. International Colloquium on Stability and Ductility of Steel Structures 2006, Vol. 1*. 863-870.

Steel Deck Instituute. (2011). “C-2011 Standard for composite steel floor deck-slabs”.

Titoum, M., Mazoz, A., Benanane, A. & Ouinas, D. (2016). “Experimental study and finite element modelling of push-out test on a new shear connector of I-shape”. *Advanced Steel Construction.* **12**(4), 487-506.

Wehbe, N., Wehbe, A., Dayton, L. & Sigl, A. (2011). “Development of concrete/cold formed steel composite flexural members”. *In ASCE Structures Congress 2011*, 3099-3109.